Journal of Hazardous Materials 209–210 (2012) 293–298

Contents lists available at SciVerse ScienceDirect

Journal of Hazardous Materials

journal homepage: www.elsevier.com/locate/jhazmat

Scaling of surface-plasma reactors with a significantly increased energy density for NO conversion

Muhammad Arif Malik*, Shu Xiao, Karl H. Schoenbach

Frank Reidy Research Center for Bioelectrics, Old Dominion University, 4211 Monarch Way, Suite 300, Norfolk, VA 23508, USA

ARTICLE INFO

Article history:
Received 24 October 2011
Received in revised form
22 December 2011
Accepted 6 January 2012
Available online 20 January 2012

Keywords:
Scaling of reactor
Nitric oxide
Non-thermal plasma
Surface-plasma
Flue gas treatment
NO_x removal

ABSTRACT

Comparative studies revealed that surface plasmas developing along a solid–gas interface are significantly more effective and energy efficient for remediation of toxic pollutants in air than conventional plasmas propagating in air. Scaling of the surface plasma reactors to large volumes by operating them in parallel suffers from a serious problem of adverse effects of the space charges generated at the dielectric surfaces of the neighboring discharge chambers. This study revealed that a conductive foil on the cathode potential placed between the dielectric plates as a shield not only decoupled the discharges, but also increased the electrical power deposited in the reactor by a factor of about forty over the electrical power level obtained without shielding and without loss of efficiency for NO removal. The shield had no negative effect on efficiency, which is verified by the fact that the energy costs for 50% NO removal were about 60 eV/molecule and the energy constant, k_E, was about 0.02 L/J in both the shielded and unshielded cases.

1. Introduction

Atmospheric pressure, nonthermal plasma channels (streamers) are formed when high voltage pulses of short duration and short rise time are applied to electrodes which generate highly nonuniform fields, such as wire-to-cylinder or wire-to-plate electrodes. The streamers originate from the thin wire electrode and propagate toward the counter electrode. The presence of any dielectric surface in the path of the streamers causes a redistribution of the electric fields in such a way that the streamers attach to the surface and propagate along the solid–gas interface, as in the case of surface-flashover [1,2]. The plasma generated by streamers in the gas (not in contact with dielectric materials) is called volume plasma; the plasma generated by streamers at a solid–gas interface is called surface plasma in this report.

One application for pulsed corona discharges and other nonthermal atmospheric pressure plasmas, such as dielectric barrier discharges, is air pollution abatement [3–5]. Our previous studies revealed that surface plasma is more effective and energy efficient than volume plasma for destruction of toxic volatile organic compounds (VOCs) [6] and conversion of nitric oxide (NO) from air [7,8]. The increased efficiency of surface plasmas was assumed to be due to surface-mediated reactions. This assumption was supported by the observation that the streamer propagation in the surface discharges and the NO removal efficiency are dependent on the type of dielectric [2,7]. In the case of NO conversion, such surface-mediated reactions are adsorption and stabilization of atomic oxygen followed by the reaction of the adsorbed radicals with NO to form NO_2 [9]. Our results are in agreement with the results reported by other researchers for similar experimental conditions. For example, more energy efficient destruction of VOCs [10], conversion of NO [11], and ozone synthesis [12] has been reported for nonthermal discharges where the electrodes were in contact with the dielectric surface (surface plasma) compared to the cases where the electrodes were separated from the dielectric surface (volume plasma).

Nitric oxide (NO) to nitrogen dioxide (NO_2) conversion by nonthermal plasmas is being developed as part of a system for the abatement of nitrogen oxides (NO_x) from flue gases and diesel engine exhausts [3,13–20]. NO_2 would, in this case, be removed by another technique, e.g., by selective catalytic reduction [3,13,14], adsorption [15,16], or dissolution in water followed by reduction [17,18]. Selective catalytic reduction of NO with ammonia is possible, but this technique is more effective when NO and NO_2 are in 1–1 molar ratio [21]. Based on lower energy cost, the surface plasma reactor is considered to be a prime candidate for the NO into NO_2 conversion in an integrated abatement system.

Scaling of the surface plasma reactors to large volumes by operating them in parallel suffers from a serious problem of adverse effects due to the formation of surface charges at the surface of the dielectric which separates the chambers [22]. This study revealed

* Corresponding author.
E-mail address: MArifMalik@gmail.com (M.A. Malik).

0304-3894/$ – see front matter © 2012 Elsevier B.V. All rights reserved.
doi:10.1016/j.jhazmat.2012.01.024

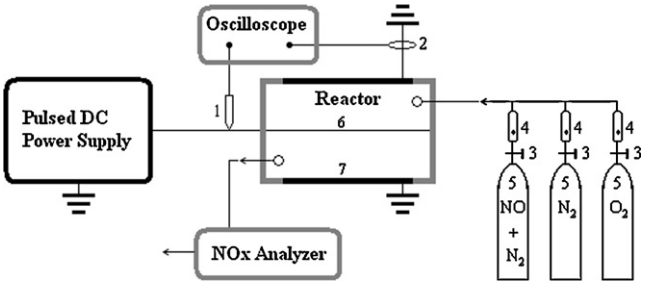

Fig. 1. Schematics of the experimental setup: 1 is the voltage probe, 2 is the current probe, 3 are needle valves, 4 are gas flow meters, 5 are pressurized gas bottles, 6 is the anode (wire), and 7 is the cathode.

that electrical shielding between the discharge reactors is required to avoid the adverse effects. The shield not only decoupled the neighboring plasmas, it increased input electrical power by a factor of about fifty. The factors responsible for these positive effects of the shield are described.

2. Experimental

The schematic of the experimental setup is illustrated in Fig. 1. High voltage pulses of positive polarity were delivered by a "Compact Pulsed Power Modulator MPC3000S-OP1" (Suematsu Electronics Co., Ltd., Japan) to the wire electrode (anode). The pulse repetition rate was varied in the range of 1–500 Hz, with an applied peak voltage of 30 kV in all experiments except when mentioned otherwise. The setup for the voltage and current diagnostics and the procedure for estimating the power consumption were the same as described in Refs. [6–8], using a Tektronix TDS 3052 oscilloscope, a Tektronix P6015A voltage probe and a Pearson Electronics Current Monitor, Model 110A. The instant power was calculated from the product (VI) of the measured pulse voltage (V) and current (I). The energy per pulse (E_p) is the time integral ($\int VI\,dt$) of the power. The displacement current was measured by reducing the applied voltage to values below that required for the discharge breakdown or plasma formation. The typical values of the electrical parameters are listed in Table 1.

Two surface plasma reactors employed in this study are shown in Fig. 2. The two reactors (unshielded Fig. 2b and shielded Fig. 2c) are identical, except that in the case of the shielded reactor the two cathodes are connected through aluminum foil (shield) which covers the entire area of the glass sheet onto which, on the opposite side, the anode wire is placed. In some experiments two discharge chambers were stacked and operated in parallel as shown in Fig. 2d.

The electric potential distribution in the two reactors was modeled by a 3-D electrostatic Poisson equation solver, Amaze-3D (Field Precision, Albuquerque, NM). A voltage of 1 kV was applied between the wire and ground electrodes. In the modeling, the diameter of the wire is not the same as in the real reactors, so the result does not show an exact potential distribution but a qualitatively similar picture.

Table 1
Electrical characteristic of high voltage pulses employed in this study.[a]

Reactor	Peak current (A)	Energy per pulse[b] (mJ)
Without shield (Fig. 2b)	5	1.6 ± 0.2
Without shield two parallel	5	1.4 ± 0.1
Shielded (Fig. 2c)	70	64 ± 1
Shielded two parallel (Fig. 2d)	105	92 ± 1

[a] Peak voltage ~30 kV, rise time of the voltage (10–90%) ~50 ns and pulse width at half maximum ~100 ns were common in all the cases.
[b] Average values ± standard deviations.

Gases, i.e., N_2, O_2 and NO, were supplied from gas cylinders. The flow rates of the gases were controlled by needle valves and monitored with ball-float flow meters. The process gas was ~300 ppm NO balance air with 20.1% oxygen at one atmosphere of pressure and 25 °C, flowing at a rate of 1 liter per minute (L/min) through the discharge chamber, except when mentioned otherwise. Two discharge chambers were operated in parallel electrically and the gas flow was also parallel, i.e., 1 L/min through each chamber with a total flow rate of 2 L/min.

The concentrations of O_2, and NO were monitored by a NO_x analyzer (ENERAC Model 500), equipped with O_2, and NO sensors. The resolution of the O_2 and NO sensors was 0.1%, and 1 ppm, respectively, and their accuracy, as specified by the manufacturer, was 0.2%, and 4% of the reading, respectively. Laboratory testing with N_2/O_2, NO/N_2, and $NO/NO_2/N_2$ mixtures show the accuracies for O_2 and NO measurements were well within the limits specified by the manufacturer. To get stable inlet NO concentration (NO_{in}), the process gas was allowed to flow for one hour before the discharge was switched ON. The outlet NO concentrations (NO_{out}) were monitored inline and recorded for 3 min duration after 15 min of discharge ON. The standard errors during the 3 min of measurements are not shown in the figures as error bars because they were smaller than the size of the symbols shown in the figures.

Conversion of NO is expressed as a percentage (%) calculated by means of the formula:

$$\text{NO Conversion} = 100\left(\frac{NO_{out}}{NO_{in}}\right), \quad (1)$$

where NO_{out} and NO_{in} are the NO concentration at reactor outlet and inlet, respectively, both are given in ppm. The power consumed in the reactor (W) in J/s was calculated by means of the formula:

$$W = E_p f, \quad (2)$$

where E_p is the energy per pulse in Joules (J) and f is frequency or repetition rate in Hertz (Hz). The specific input energy (SIE) in joules per liter (J/L) was calculated by using the formula:

$$\text{SIE} = \frac{W}{Q}, \quad (3)$$

where Q is flow rate of the process gas in liters per second (L/s). The energy cost (EC) in units of electron-volts per NO molecule (eV/molecule) was calculated using the formula [23]:

$$\text{EC} = \frac{250(\text{SIE})}{NO_{in} - NO_{out}}, \quad (4)$$

The energy constant (k_E in units of L/J) under the condition SIE <60 eV/molecule was calculated as a slope of the curve from the following equation [8,24]:

$$\ln\left(\frac{NO_{out}}{NO_{in}}\right) = -k_E(\text{SIE}). \quad (5)$$

3. Results

Four arrangements of discharge chambers, i.e., a single and two chambers in parallel without any electric shield, and a single and two chambers in parallel, but shielded, were compared. The energy per pulse in the single discharge chamber without a shield was 1.6 mJ. Contrary to an expected increase, the energy per pulse in the dual discharge chambers without shielding was almost the same as in the single discharge chamber without shielding. The energy per pulse increased to 64 mJ in a shielded single discharge chamber and to 92 mJ in the shielded dual discharge chamber. The specific input energy increased sharply in the shielded discharge chamber compared to the cases without shield, when the pulse repetition rate and applied voltage was increased as shown in Fig. 3. The experiments in the single shielded discharge chamber were repeated in

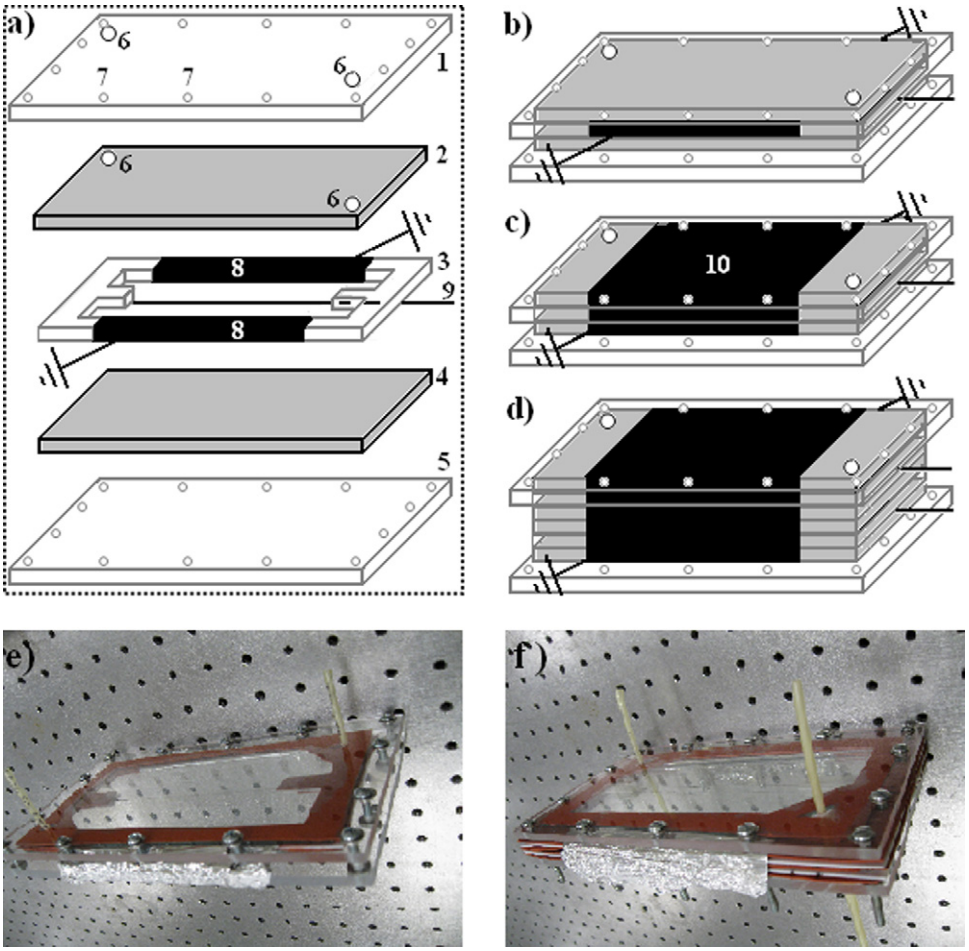

Fig. 2. Surface discharge chamber between two glass sheets with wire-to-strip-shaped electrodes stretched on one of the glass sheet surfaces (a) is a partially expanded view, (b) is a view of the assembled device (reactor without shield), (c) is the view of the same assembled device as in 'b' with the area of the aluminum foil which is used for the cathodes being extended by wrapping it on the outer sides of glass sheets# 2 and 4 (shielded reactor), (d) is the shielded reactor having two discharge chambers operated in parallel (layers: 1-shield-2-3-4-shield-2-3-4-shield-5), (e) is an image of one discharge chamber without shield, and (f) is image of two-parallel discharge chambers without shield. The components are: 1 and 5 are top and bottom Plexiglas sheets used to hold the dielectric layers and electrodes; 2 and 4 are top and bottom dielectric layers (soda-glass sheets), 22 cm × 13 cm × 0.3 cm; 3 is a Teflon spacer of 0.2 cm thickness and 2.5 cm stripe on each side; 6 are gas inlet/outlet; 7 are holes for nuts and bolts; 8 are two cathodes made of aluminum foil of 150 μm thickness and 13 cm effective length (wrapped around the sides of the spacer) and separated from the anode by a gap of 4 cm; 9 is stainless steel wire anode of 150 μm diameter; and 10 is a grounded aluminum foil of 13 cm width wrapped on the outer sides of the glass sheets. Gas leakage was prohibited by using silicon sealant.

a second, identical shielded reactor. Fig. 3a shows that the reproducibility of the results was reasonably good for our experimental conditions.

Fig. 4 shows the comparison of NO conversion in the various discharge chambers. The NO conversion at a pulse repetition rate of 40 Hz was ≥80% in the single-shielded and dual-shielded discharge chambers. The result is significantly higher than the ≤10% conversion by the single discharge and the dual discharges without shielding under the same experimental conditions. The maximum NO conversion achieved without the shield was ~60% in the

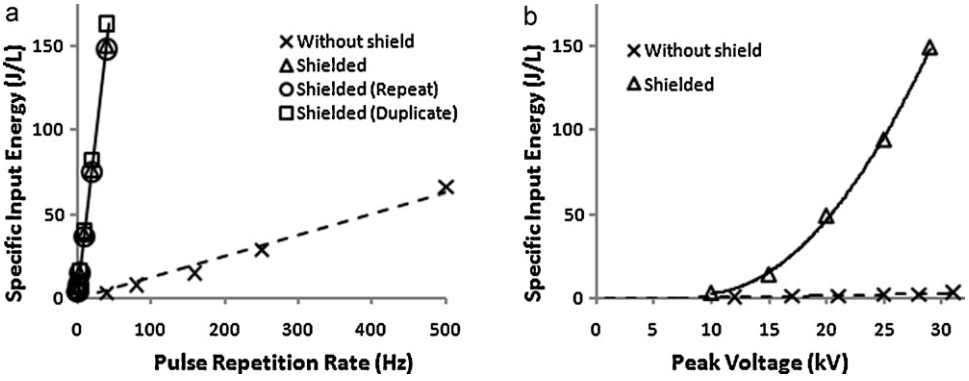

Fig. 3. Specific input energy (energy density) curves with respect to (a) pulse repetition rate at 30 kV peak voltage and (b) peak applied voltage at 40 Hz, for a single discharge chamber without shield (crosses) and a shielded chamber (triangles, circles and squares).

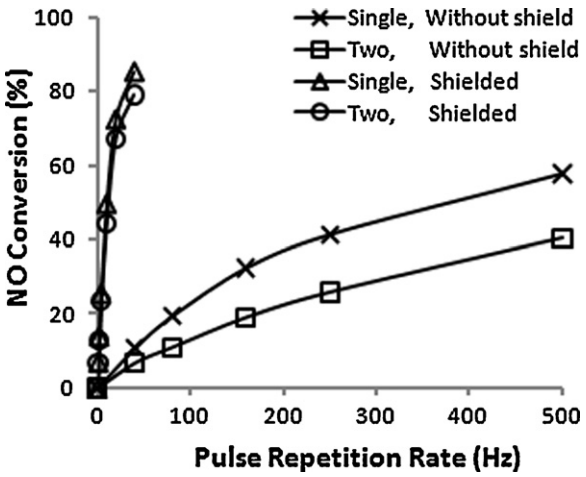

Fig. 4. NO conversion versus pulse repetition rate curves for single and two-parallel discharge chambers with and without shielding. Peak voltage was ~30 kV and NO concentration was ~300 ppm.

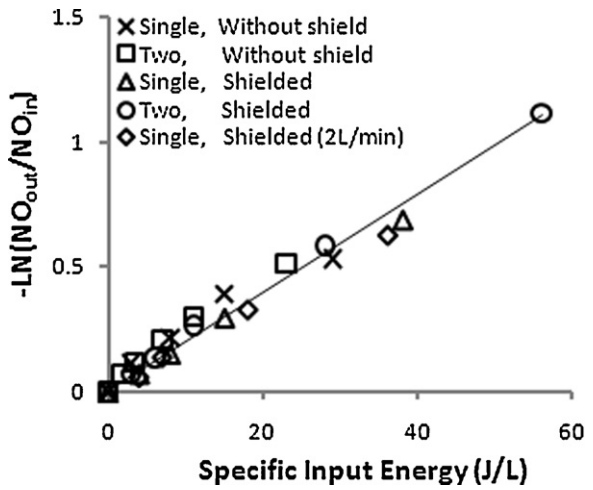

Fig. 6. Semi-log plot of data based on Eq. (5) for different conditions shown in Fig. 5 under the condition: specific input energy <60 J/L.

single discharge chamber and ~40% in the dual discharge chambers at a pulse repetition rate of 500 Hz. Plasma treatment converts NO in dry air mainly into NO_2 [13–20]. However, NO_2 concentrations are not shown because the accuracy of NO_2 analysis by the NO_x analyzer employed in this study was poor.

Fig. 5 shows that NO conversion is mainly determined by specific input energy which is in accordance with the conclusion drawn from reviews of earlier literature [24]. The energy cost at 50% NO removal (EC_{50}) was ~60 eV/molecule in all cases compared in this study. These results show that the plasma reactor with or without shielding and operated in single-chamber or dual-chamber mode is almost equal with respect to rates of NO conversion and energy cost for NO conversion.

Fig. 6 shows that Eq. (5) provided a good fit to the measured data under the condition of the specific input energy being <60 L/J, which is in accordance with earlier studies [24]. The coefficient of determination (R^2) was 0.96 which is close enough to 1 to confirm that the equation provided a good fit. The energy constant k_E indicates the efficiency of the reactor: higher k_E means better efficiency. The k_E was ~0.02 L/J in all cases in this study, which is the same value as in the case of surface plasma [8] and better than the k_E of 0.011 L/J [24] reported in earlier literature where volume plasmas were formed by positive pulsed corona discharges for the same concentration of NO (300 ppm) in dry air.

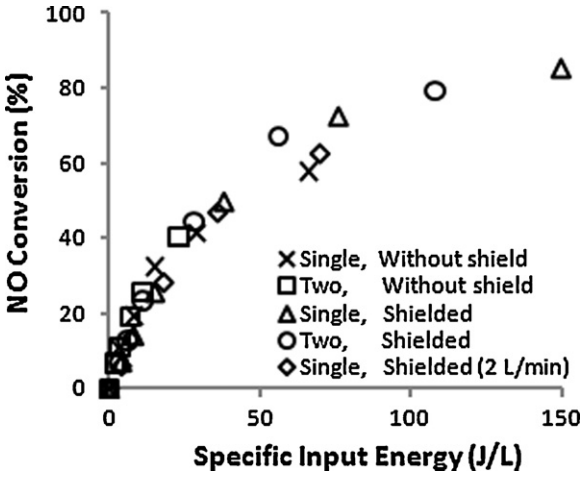

Fig. 5. NO conversion versus specific input energy curves for single and two-parallel discharge chambers with and without shielding. Flow rate of the process gas was 1 L/min except in the case of the single shielded discharge chamber where both 1 L/min and 2 L/min were employed. Other experimental conditions were the same as in Fig. 4.

Fig. 7 shows modeling results of the electric potential distribution in the two discharge chambers. The potential distribution in the discharge chamber without shielding is shown in Fig. 7a. The potential lines spread not only into the electrode gap, but also leak through the glass dielectric, coupling to a second reactor placed below the glass. On the other hand, in the shielded discharge chamber, adding an aluminum foil confines all the potential lines within the reactor, thereby totally decoupling it from the neighboring reactor, as shown in Fig. 7b. It should be noted that when we modeled the potential distribution, because of symmetry reasons, only half of the reactor was modeled. In the real structure, a glass sheet is placed on top of the modeled reactor also. This glass, however, will affect the potential distribution only slightly, since it is further removed from the dielectric on which the electrodes are placed. In the modeled structure of the shielded reactor (Fig. 7b), it is obvious that adding a top ground electrode will confine all the potential lines and, consequently, the electric field, entirely within the reactor.

4. Discussion

The electrode configuration with the center steel wire (anode) and the two strips (cathodes) at the opposite sides generates discharges which are only slightly influenced by the presence of the dielectric beneath the electrodes. The pulsed dc discharge plasma will generate a positive surface charge on the dielectric surface [25] and consequently create a normal component of the electric field that accelerates the electrons toward the surface. However, the redistribution of the electric field is still less than in the case where the cathodes are connected by a conductive layer (shield) on the rear side of the dielectric layer. In this case, even without surface charge, the electrode arrangement causes a strong increase in the component normal to the surface of the dielectric that can be inferred from Fig. 7. The effect is strongest at the wire where the electric field intensity is highest, as shown in Fig. 7b. This fosters the ignition of breakdown and a more homogeneous distribution of the streamers. In addition, the streamer plasma generates, as in any surface discharge, a positive space charge on the dielectric [25]. The application of electric fields in the presence of the conductive layer polarizes the dielectric and creates surface charges that lead to a strong electric field component normal to the surface.

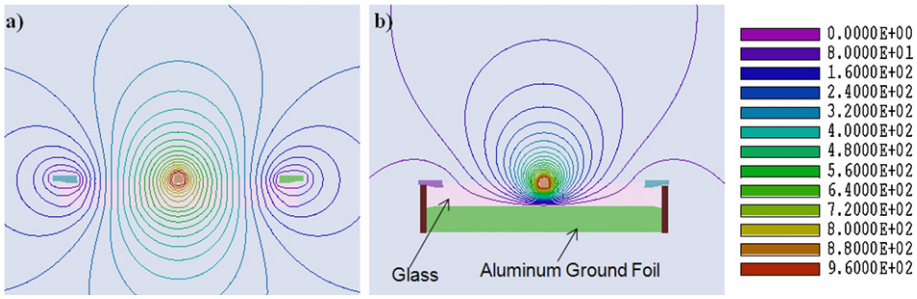

Fig. 7. Side views of electric potential distribution of rectors compared in this study (a) is a discharge chamber without shield and (b) is a shielded discharge chamber.

The normal field component accelerates free electrons to the surface and keeps the plasma attached to the surface. It results in increased rates of secondary electron emission through thermionic emission or photoemission from the surface [1]. This effect explains the increase in electrical power deposited in the plasma and the increase in rates of chemical reactions in the presence of the shield, as compared to the case without a shield. These results are in accordance with a similar increase in input energy and efficiency reported in the literature, in the case of the laser pumping application of sliding surface discharges [26].

It is known that the surface plasma in one discharge chamber has an adverse effect on the plasma formation in the neighboring discharge chamber operating in parallel [22]. The effect is probably due to the space charge layer on the dielectric surfaces, which induces charges of opposite polarity on the opposite side of the dielectric surface. This hypothesis explains the lack of an increase in electrical power when two surface plasma rectors sharing a common dielectric layer are operated in parallel, as compared to single reactor. By placing the conductive layer around the discharge gap, the space charge effects are eliminated. The two reactors are completely isolated from each other even though they share the same ground, which makes it possible to stack a large number of reactors without electrically interfering with each other. This can be concluded from the modeling results of electric potential distribution in the two reactors as shown in Fig. 7.

Surface plasma reactors, such as those employed in this study, have an additional advantage over the conventional volume plasma reactors due to the increased role of surface-mediated reactions [7,8]. For example, recent literature shows that atomic oxygen is adsorbed and stabilized on dielectric surfaces and it becomes available for reactions with NO for hours after the adsorption through the following surface-mediated reactions [9]:

$$O \rightarrow O_{ads}, \quad (6)$$

$$O_{ads} + NO \rightarrow NO_2. \quad (7)$$

Similarly, the adsorption and stabilization of atomic nitrogen followed by its utilization in surface mediated reactions has also been reported in recent literature [27].

The surface plasma concentrated at the dielectric surfaces favors surface-mediated reactions. It also results in a more homogeneous distribution of the plasma and better mixing of the reactants in the discharge gap compared with coaxial electrodes in conventional volume-plasma reactors [10]. Introduction of the shield results in a stronger attachment of the plasma with the surface [26] that may promote the surface mediated reactions. Another advantage of the surface plasma reactor is that there is no change in NO conversion with increase in energy per pulse by shielding but keeping the same specific input energy. In conventional volume plasma the increase in energy per pulse without varying specific input energy drastically decreases the rate of NO removal [28].

Further improvements in the surface plasma reactors employed in this study can be expected when the surface area of the dielectric in contact with the plasma is increased, e.g., by depositing a layer of a porous ceramic on the dielectric layer. This will allow the full realization of the benefits of adsorption and stabilization of the chemically active species on the surface. As a further control over the plasma chemistry, catalysts can be used which can be supported on the porous ceramic layer.

5. Conclusion

It is clear from the results that the electric shielding in the surface plasma reactors allows a significant increase in specific input energy without losing efficiency for NO conversion. Higher specific input energy is desirable for practical applications, since it allows treatment of larger volumes of the process gas in a given volume of the discharge chamber. Furthermore, the shielded reactor is scalable by stacking and operating multiple discharge chambers in parallel.

Acknowledgements

This work is supported by the “Frank Reidy Fellowship in Environmental Plasma Research” and with internal funds of the Frank Reidy Research Center for Bioelectrics.

References

[1] V. Bloshchitsyn, Review of Surface Discharge Experiments, 2010, http://arxiv.org/abs/1005.5044v1.
[2] N.L. Allen, P.N. Mikropoulos, Streamer propagation along insulating surfaces, IEEE Trans. Dielect. Electr. Insul. 6 (1999) 357–362.
[3] J.O. Chae, Non-thermal plasma for diesel exhaust treatment, J. Electrostat. 57 (2003) 251–262.
[4] L.A. Rosocha, Nonthermal plasma applications to the environment: gaseous electronics and power conditioning, IEEE Trans. Plasma Sci. 33 (2005) 129–137.
[5] J.V. Durme, J. Dewulf, C. Leys, H.V. Langenhove, Combining non-thermal plasma with heterogeneous catalysis in waste gas treatment: a review, Appl. Catal. B: Environ. 78 (2007) 324–333.
[6] M.A. Malik, Y. Minamitani, K.H. Schoenbach, Comparison of catalytic activity of aluminum oxide and silica gel for decomposition of volatile organic compounds (VOCs) in a plasmacatalytic reactor, IEEE Trans. Plasma Sci. 33 (2005) 50–56.
[7] M.A. Malik, K.H. Schoenbach, A novel pulsed corona discharge reactor based on surface streamers for NO conversion from N_2–O_2 mixture gases, Int. J. Plasma Environ. Sci. Technol. 5 (1) (2011) 50–57.
[8] M.A. Malik, J.F. Kolb, Y. Sun, K.H. Schoenbach, Comparative study of NO removal in surface-plasma and volume-plasma reactors based on pulsed corona discharges, J. Hazard. Mater. 197 (2011) 220–228.
[9] O. Guaitella, M. Hubner, S. Welzel, D. Marinov, J. Ropcke, A. Rousseau, Evidence for surface oxidation on pyrex of NO into NO_2 by adsorbed O atoms, Plasma Sources Sci. Technol. 19 (2010) 045026.
[10] L. Oukacine, J.M. Tatibouet, J. Jolibois, E. Moreau, Ionic wind effect on the chemical reactivity, in: Int. Symp. Non-Thermal/Thermal Plasma Pollut. Control Technol. & Sustainable Energy, St. John’s, Newfoundland, Canada, June 21–25, 2010.
[11] E. Odic, M. Dhainaut, M. Petit, C. Karimi, A. Goldman, M. Goldman, Towards a better understanding of the electrical parameters monitoring the chemical reactivity of dielectric barrier discharges at atmospheric pressure, in: Proc.

3rd Int. Symp. Non-Thermal Plasma Technol. Pollut. Control, Seogwipo, Cheju Island, Republic of Korea, 2001, pp. 62–67.
[12] E. Odic, M. Dhainaut, M. Petit, A. Goldman, M. Goldman, C. Karimi, Approach of the physical and chemical specific properties of pulsed surface dielectric barrier discharges in air at atmospheric pressure, J. Adv. Oxid. Technol. 6 (2005) 41–47.
[13] S.Y. Park, B.R. Deshwal, S.H. Moon, NO_x removal from the flue gas of oil-fired boiler using a multistage plasma-catalyst hybrid system, Fuel Process. Technol. 89 (2008) 540–548.
[14] Y. Itoh, M. Ueda, H. Shinjoh, K. Nakakita, M. Arakawa, NO_x reduction under oxidizing conditions by plasma-assisted catalysis, R&D Rev. Toyota CRDL 41 (2) (2006) 49–62.
[15] A. Mihalcioiu, K. Yoshida, M. Okubo, T. Kuroki, T. Yamamoto, Design factors for NO_x reduction in nitrogen plasma, IEEE Trans. Ind. Appl. 46 (6) (2010) 2151–2156.
[16] S. Mohapatro, S.B. Rajanikanth, Cascaded cross flow DBD-adsorbent technique for NO_x abatement in diesel engine exhaust, IEEE Trans. Dielectr. Electr. Insul. 17 (5) (2010) 1543–1550.
[17] T. Yamamoto, H. Fujishima, M. Okubo, T. Kuroki, Pilot-scale NO_x and SO_x removal from boiler emission using indirect-plasma and chemical hybrid process, IEEE Trans. Ind. Appl. 46 (1) (2010) 29–37.
[18] S.M. Thagard, Y. Kinoshita, H. Ikeda, K. Takashima, S. Katsura, A. Mizuno, NO_3^- reduction for NO_x removal using wet-type plasma reactor, IEEE Trans. Ind. Appl. 46 (6) (2010) 2165–2171.
[19] X.Q. Wang, Y. Li, W. Chen, G.H. Lv, J. Huang, G.X. Zhu, X.Q. Wang, X.H. Zhang, D.C. Wang, K.C. Feng, S.Z Yang, Characteristics of NO_x removal combining dielectric barrier discharge plasma with selective catalytic reduction by C_3H_6, Jpn. J. Appl. Phys. 49 (2010) 086201.
[20] H. Barankova, L. Bardos, Effect of the electrode material on the atmospheric plasma conversion of NO in air mixtures, Vacuum 84 (2010) 1385–1388.
[21] Y.H. Lee, J.W. Chung, Y.R. Choi, J.S. Chung, M.H. Cho, W. Namkung, NO_x removal characteristics in plasma plus catalyst hybrid process, Plasma Chem. Plasma Process. 24 (2004) 137–154.
[22] J. Furmanski, J.Y. Kim, S.O. Kim, Triple-coupled intense atmospheric pressure plasma jet from honeycomb structural plasma device, IEEE Trans. Plasma Sci. 39 (2011) 2338–2339.
[23] M. Gundersen, V. Puchkarev, A. Kharlov, G. Roth, J. Yampolsky, D. Erwin, Transient plasma-assisted diesel exhaust remediation, in: R. Hippler, H. Kersten, M. Schmidt, K.H. Schoenbach (Eds.), Low Temperature Plasmas. Fundamentals, Technologies, and Techniques, 2nd ed., Wiley-VCH Verlag GmbH, Weinheim, 2008, pp. 543–550.
[24] H.H. Kim, G. Prieto, K. Takashima, S. Katsura, A. Mizuno, Performance evaluation of discharge plasma process for gaseous pollutant removal, J. Electrostat. 55 (2002) 25–41.
[25] A. Kumada, S. Okabe, K. Hidaka, Residual charge distribution of positive surface streamer, J. Phys. D: Appl. Phys. 42 (2009), 095209 (8pp.).
[26] G.N. Tsikrikas, A.A. Serafetinides, The effect of voltage pulse polarity on the performance of a sliding discharge pumped HF laser, J. Phys. D: Appl. Phys. 29 (1996) 2806–2810.
[27] D. Marinov, O. Guaitella, A. Roussseau, Y. Ionikh, Production of molecules on a surface under plasma exposure: example of NO on pyrex, J. Phys. D: Appl. Phys. 43 (2010) 115203.
[28] A. Khacef, J.M. Cormier, J.M. Pouvesle, Energy deposition effect on the NO_x remediation in oxidative media using atmospheric non thermal plasmas, Eur. Phys. J. Appl. Phys. 33 (2006) 195–198.